Volume 80, March 2014 ISSN 0010-938X

ELSEVIER

CORROSION SCIENCE

The Journal on Environmental Degradation of Materials and its Control

Editor-in-Chief: G. T. BURSTEIN, University of Cambridge, U.K.

An Official Journal of the Institute of Corrosion

CONTENTS

Contents continued on outside back cover

http://www.elsevier.com/locate/corsci

Corrosion Science 80 (2014) 197–204

Contents lists available at ScienceDirect

Corrosion Science

journal homepage: www.elsevier.com/locate/corsci

EIS assessment of critical pitting temperature of 2205 duplex stainless steel in acidified ferric chloride solution

M. Hoseinpoor [a], M. Momeni [a], M.H. Moayed [a,*], A. Davoodi [b]

[a] Metallurgical and Materials Engineering Department, Faculty of Engineering, Ferdowsi University of Mashhad, Mashhad 91775-1111, Iran
[b] Materials Engineering Department, Hakim Sabzevari University, Sabzevar, Iran

ARTICLE INFO

Article history:
Received 15 August 2013
Accepted 19 November 2013
Available online 23 November 2013

Keywords:
A. Stainless steel
B. EIS
B. Polarisation
C. Pitting corrosion

ABSTRACT

In this study, critical pitting temperature (CPT) of 2205 duplex stainless steel (DSS2205) was assessed using electrochemical impedance spectroscopy (EIS) in ferric chloride solution. In order to verify the results other methods such as ASTM G 48, potentiodynamic and potentiostatic polarisation and zero resistance ammeter (ZRA) were also employed. The results show a strong close relation between the results of this method by those of previous methods. CPT of the alloy is 40 °C based on standard method and 44 °C, 49 °C according to the ZRA and potentiostatic methods. Both potentiodynamic and EIS methods give an almost identical CPT value.

1. Introduction

Temperature as a pitting criterion first introduced by Brigham and Tozer [1]. They compared the results of the three independent test methods (two potentiostatically controlled and one freely corroding) on austenitic stainless steels for describing the onset of pitting corrosion in chloride containing solutions [1–4]. They reported that there is a temperature below which the steels will not pit regardless of potential and exposure time and introduced it as the critical pitting temperature (CPT). This temperature is an important parameter for selection of pitting resistance of stainless steels. In this way, the higher CPT value shows the better resistance of stainless steel to pitting corrosion.

It is generally accepted that the alloy elements are one of the most effective factors on the CPT values [2,4–6]. In addition, some other factors such as surface roughness, heat treatment and some inhibitors can also change CPT values [7–12]. However, it is believed that the potential and chloride concentration with in a lower concentration range have negligible influence on the CPT [1,13].

To determine CPT values different methods have been reported by authors that are listed below:

A. Brigham and Tozer in 1973 used potentiostatic polarisation to determine CPT values of molybdenum-containing austenitic stainless in 3.5% NaCl solution [1]. They applied an anodic potential of 500 mV/SCE on their samples while the solution temperature was increased at the rate of 0.6 °C min^{-1}. The temperature at which current density increased sharply to 100 μA cm^{-2} was designated as the critical pitting temperature. In addition, according to ASTM G 150 test, CPT values of stainless steels can be determined by potentiostatic polarisation [14]. In this test, an anodic potential of 700 mV/SCE applies on sample in 1 M NaCl solution while the temperature increases at the rate of 1 °C min^{-1}. The temperature at which current reaches to 100 μA cm^{-2} and continues for more than 1 min is designated as the critical pitting temperature.
B. ASTM G 48 in 1976 issued as a standard test method for pitting and crevice corrosion resistance of stainless steels and related alloys by use of ferric chloride solution [15]. According to this method sample is retained in acidified 6–10% $FeCl_3$ solution at an initial temperature (usually 10 °C below the expected CPT) for 24 h. After this duration sample is examined under optical microscopy to detect any pitting. The critical pitting temperature is designated as the temperature below which no pits are observed. In addition, according to ASTM G 48 the depth of the formed pits must be higher than 25 μm.
C. Quang et al. in 1988 introduced galvanostatic polarisation as a fast method for determination of critical pitting temperature [16]. They applied a weak anodic current density (50–200 μA cm^{-2}) to prepassivated samples (5 min in 3 N Nitric acid) in 3% NaCl solution while the temperature was increased at the rate of lower than 4 °C min^{-1}. The

* Corresponding author. Tel.: +98 5118763305; fax: +98 5118763301.
E-mail address: mhmoayed@um.ac.ir (M.H. Moayed).

0010-938X/$ - see front matter © 2013 Elsevier Ltd. All rights reserved.
http://dx.doi.org/10.1016/j.corsci.2013.11.023

temperature at which the potential dropped suddenly due to stable pitting formation was designated as the critical pitting temperature.

D. Qvarfort in 1989 proposed an improved electrochemical method based on potentiodynamic polarisation to determine critical pitting temperature of stainless steels [17]. The cell design avoided the crevice corrosion and resulted to accurate determination of the critical pitting temperature. In this method, the temperature at which the breakdown potential, E_b, felt down sharply from transpassive to pitting corrosion and the current density exceeded 100 μA cm^{-2} was designated as the critical pitting temperature.

E. Bravo and Newman in 1994 proposed zero resistance ammeter (ZRA) as an alternative method to determine critical pitting temperature of stainless steels in ferric chloride solution [18]. In this method, potential and coupled current between to samples was being monitored while the temperature was increased by defined rate. The temperature at which coupled current increased to a value of ±5 μA was designated as the critical pitting temperature.

F. Zhang et al. in 2012 proposed a new criterion to estimate critical pitting temperature based on the electrochemical noise measurement [19]. In this procedure, electrochemical noise recorded during the temperature linear scanning period which is analyzed by the thermammetry technique. Afterward, the temperature of transition point in Arrhenius plot was designated as the critical pitting temperature.

G. Ebrahimi et al. in 2012 proposed electrochemical impedance spectroscopy (EIS) as a fast and reliable method to determine critical pitting temperature of the stainless steels [20]. In this method, nyquist plots of the sample in 0.1 M NaCl at the anodic potential of 600 mV/SCE in different temperature were plotted. The temperature at which sudden drop in charge transfer resistance occurred was designated as the critical pitting temperature.

As known, the CPT determination by ASTM G 48 evaluation is a qualitative and time-consuming process. Generally, it is expected that at temperature above the CPT the stable pitting will occur in ferric chloride solution approximately after a short time and it is not necessary to immerse the sample into solution for a longer time. In present study, this expectation has been investigated by impedance measurement. In this way, the CPT is estimated by EIS method using an oxidizing environment (acidified ferric chloride solution) instead of applying anodic potential in conjunction with impedance spectroscopy that was previously employed by Ebrahimi et al. [20]. Finally several CPT measurement techniques including ASTM G 48, ZRA, potentiodynamic and potentiostatic polarisation are employed to determine CPT value of the 2205 duplex stainless (DSS2205) and their results are compared with value obtained by proposed method.

2. Experimental procedure

The chemical composition analysis of alloy in weight percent is illustrated in Table 1. The samples have been solution annealed at the temperature of the 1050 °C for 45 min and quenched in water. In this case to avoid crevice corrosion, rod samples with 10 mm diameter and 20 mm length were used. The immersion depth of working electrode was 12 mm; therefore, the immersion surface area was 4 cm^2. Prior to each experiment, the sample was wet ground to 1200-grit finish by abrasive paper, degreased with methanol, rinsed with distilled water and dried by air. A platinum foil and a saturated calomel electrode (SCE) were used as counter and Reference electrodes, respectively and Gill AC potentiostat (ACM instruments) was employed for electrochemical measurements. Since the ferric chloride solution (prepared according to ASTM G 48-03 standard) makes an oxidizing environment to exceed the corrosion potential greater than the pitting potential, it does not need to apply any anodic over-potential to cause pitting. Thus in this study, electrochemical tests including ASTM G 48, ZRA and EIS techniques have been performed in ferric chloride solution without any applied external potential. As known in this solution, the chloride anions have the main role on pitting corrosion while reduction of ferric (Fe^{3+}) to ferrous (Fe^{2+}) just produce the oxidising power to keep the corrosion potential above pitting potential. So, the potentiodynamic and potentiostatic polarisation tests were carried out in a solution with same chloride concentration (without oxidizing agent) and pH value prepared by NaCl and HCl in order to validate the results obtained by mentioned techniques. It should be noted that in all electrochemical test, the chloride concentration and pH values were 1.6 M and −0.2, respectively.

2.1. ASTM G 48 CPT determination

This procedure involved immersing the sample in the acidified $FeCl_3$ solution at an initial temperature (30 °C) and retaining it in solution for 24 h period. At the end of the test the sample removed and the surface scrubbed by nylon bristle brush under running water to remove corrosion products. Then the sample was ultrasonically cleaned in methanol for 5 min and dried by air. Afterward, the sample was examined under an optical microscopy to detect any pitting. If no pits were found, temperature was increased by 5 °C every 24 h with a fresh solution and new sample until pits could be found. The temperature at which pits with 25 μm or higher depth was observed is CPT temperature.

2.2. ZRA CPT determination

This procedure involved immersing two identical samples with equal areas (4 cm^2) in the acidified $FeCl_3$ solution. The samples retained in 30 °C solution for 1 h before starting to heat up. Subsequently, the solution was heated up at the rate of 0.5 °C min^{-1} while the potential and coupled current was measured every 0.02 s with computer controlled electrochemical interface. Test stopped when the coupled current reached to 100 μA. In this case, the temperature at which coupled current altered more than 5 μA was selected as the CPT.

2.3. potentiodynamic CPT determination

This procedure involved polarisation curves, started from −100 mV below open-circuit potential at a scan rate of 1 mV s^{-1} and reversing the scan direction while the current indicated that stable pitting or transpassivity had occurred. Before the measurements, open-circuit potential in simulated solution was measured for 30 min. In this case, the temperature at which breakdown

Table 1
chemical composition of the used DSS2205 alloy (wt%).

Sample	C	Cr	Ni	Mo	S	P	Mn	Si	N	Other	Fe
DSS2205	0.03	21.61	5.31	3.07	0.0007	0.022	0.97	0.74	0.3	<0.5	Bal

potential, E_b, dropped from transpassivity to pitting potential range was designated as the CPT.

2.4. Potentiostatic CPT determination

This procedure involved polarisation of the sample at the anodic potential of 750 mV/SCE while the temperature was increased at the rate of 0.5 °C min^{-1}. Before the measurements, open-circuit potential in simulated solution was measured for 30 min. In this case, the temperature at which the current density reached 100 μA cm^{-2} and had continued for more than 1 min, was defined as the CPT.

2.5. EIS CPT determination

This procedure involved measuring the electrochemical impedance at different temperatures in the acidified $FeCl_3$ solution by applying AC signals in the range of 10 kHz–1 Hz with the amplitude of 10 mV peak-to-peak. Before the measurements, open-circuit potential in $FeCl_3$ solution was measured for 1 h. In this case, the temperature at which sudden drop in charge transfer resistance occurred was designated as the CPT.

2.6. Pit morphology

This procedure involved polishing the sample by 0.05 μm alumina slurry and then immersing it in the 6 wt% ferric chloride solution at 55 °C for 1 h. After removing the specimen from solution, the sample was ultra-sonically cleaned in methanol. Finally, the sample was electrochemically etched in 10 wt% KOH solution at the anodic potential of 2.5 V for 60 s and examined under an optical microscopy in order to investigate the pits configuration.

3. Results and discussion

3.1. ASTM G 48 CPT determination

Fig. 1 shows the formed pit after retaining the sample in the acidified $FeCl_3$ solution for 24 h at the temperature of 40 °C. In this way, by assuming the formed pit as a hemisphere, depth of pit equals to about 50 μm which is higher than the value required based on ASTM G 48 (25 μm) [15]. It means before this temperature, the cathodic reaction mentioned above come crosses with the anodic branch of steel surface dissolution in passive state and 40 °C is the lowest temperature in which in this medium pitting corrosion can be occurred. Hence, according to the definition of CPT and also ASTM G 48, CPT of DSS2205 is 40 °C.

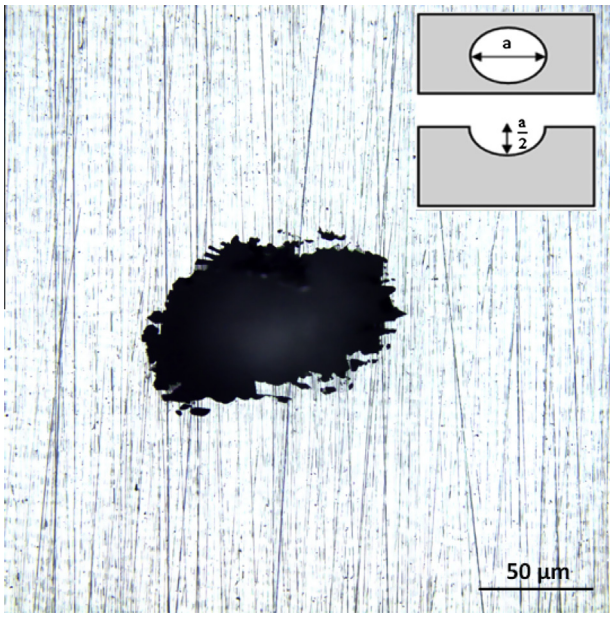

Fig. 1. Formed pit on the surface according to the ASTM G 48 at 40 °C.

3.2. ZRA CPT determination

In this method, one of the electrodes is used to promote pitting corrosion in the other one. In other word, before the CPT of the alloy, the stable pitting of the samples is not possible and both specimens are in the same corrosion potentials and the coupled current is about zero. However, by raising the temperature, formation of the metastable pits on the surfaces would be possible and it can change the potential of the samples. In this way, there will be a difference between the two specimen corrosion potentials and while they are connected electrically together, there would be a driving force for galvanic corrosion. In this galvanic couple, the specimen with a metastable pit acts as the anode and the other one would be cathode temporarily and the couple current alters proportional to the driving force. Afterward, according to the presented criterion by Bravo and Newman, the driving force from the formation of the stable pit at the CPT is high enough to alter the couple current more than 5 μA.

Fig. 2 represents the result on assessment of CPT value of the sample with ZRA measurement in the acidified $FeCl_3$ solution. Regarding couple potential, it is obvious that this potential i.e. 500 mV/SCE is located at the passive state of DSS2205 at corresponding temperatures. As a result, both samples are in passive state. Clearly, the condition remains stable since there is no noticeable change in couple current and potential values up to the 40 °C. At this temperature, the couple current density starts to decrease showing the occurrence of some changes in the surface condition. The decrease continuous until 41 °C and the couple current touches value of −4 μA; a value close to the criterion of pitting corrosion in this method. It increases again and locates at the passive boundary. The current density starts again to decrease and at 42 °C a sharp cathodic current peak with a value of 32 μA is appeared. As it can be seen from Fig. 2, the condition after that is not anymore stable and couple current density fluctuated between positive and negative values indicating formation of pits on surface of each sample. In addition, the couple potential also decreases from 500 mV/SCE to 400 mV/SCE that shows one of the samples acts

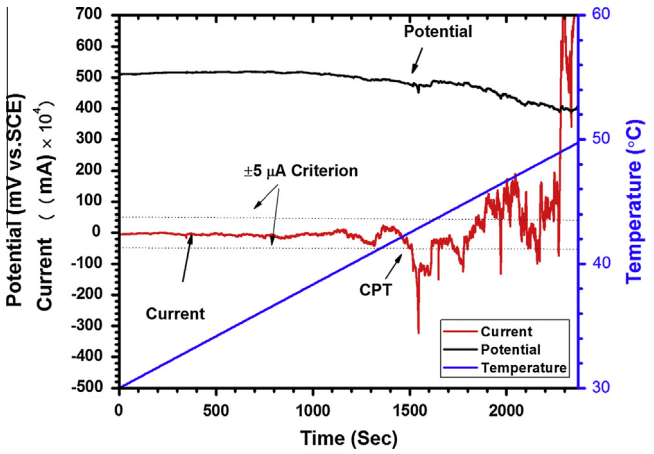

Fig. 2. Results of ZRA CPT determination method on the DSS2205. Left vertical axis shows potential (mV/SCE) and current density (10^4 mA) and right vertical axis shows temperature. Dashed horizontal lines show the current density boundary that within them no pitting corrosion is considered.

as a cathode rather than the other which is anode. According to this test, it can be claimed that 42 °C can be introduced as the CPT of this alloy.

By looking to the presented result for CPT determination by ASTM G 48 and ZRA method, a difference of about 2 °C is evident. A measured higher CPT value by ZRA method may be attributed to the different in heating process. It is believe that rate of heating is not enough low to allow the pit incubation occurs [18].

3.3. Potentiodynamic CPT determinations

In the case of potentiodynamic polarisation it is observed that the sample in the solution is in active state and by increasing the temperature from lower temperatures to higher ones, the passivity current density increases.

Fig. 3 reveals the results on assessment of CPT value of the sample with potentiodynamic polarisation in the simulated solution. It can be seen that the corrosion potential for all temperatures is between −400 to −500 mV/SCE indicating active corrosion. This behaviour is due to the low pH of aqueous environment i.e. −0.2 and by upward potential scanning the current density increases up to almost −300 mV/SCE in which the current starts to decrease.

The critical current density for the alloy by increase in temperature increases from almost 1 mA cm^{-2} to 10 mA cm^{-2}; showing the important influence of the temperature on the active corrosion of this alloy. Obviously, there is a second peak in current density after critical current density and it is seen in almost 100 mV/SCE at 25 °C and −100 mV/SCE for the other temperatures. This can be attributed to the rearranging of ions in passive film [21]. After this allotropic transformation in passive film, the current remains almost constant although there is a decrease in current (for instance, in the case of 25 °C it is up to 400 mV/SCE) and after that, it increases again until the passivity experience breakdown. The significance of the temperature on the passivity current density is noticeable. If the minimum current density in this region is considered as the passivity current density, it increases from 4 μA cm^{-2} to 40 μA cm^{-2}. It is generally accepted that by rising the temperature, the defects of the passive layer increases [22–25]. Therefore, the passive layer is less protective at higher temperatures and the passivity current density increases due to higher deficiencies of the passive film.

For all temperatures, after current density starts to increase due to transpassivity or pitting corrosion and exceeds the value of 1 mA cm^{-2}, the sweep direction is reversed to find the reason of the phenomenon. It is obvious that up to 40 °C, the reversed current density lay on the forward direction indicating transpassivity. In addition, at the presence of the localized corrosion, reversal of the scan direction results in a polarisation loop of the form shown in Fig. 3 at the temperatures 45, 50 and 55 °C. However, it can be observed that at the temperature of 45 °C the shape of the curve was different after the scan direction was reversed but the breakdown potential has not dropped sharply. In fact, while the breakdown potential is close to the previous temperatures, the backward scan shows pitting corrosion.

In this way, the current density remains abnormally high and returns to the passive current density at a lower potential. This lower-potential intersection is frequently referred to as the protection potential, E_{prot}, or repassivation potential in which the stable passive layer forms on the metal in the local pit and repassivation occurs [26,27]. The repassivation potential for the sample tested at 45 °C is almost 100 mV/SCE. The breakdown potential dropped sharply to 350 mV/SCE at 50 and 55 °C and also the repassivation potential is also decreased to almost 0.0 mV/SCE. This is an indication of pitting corrosion in temperatures 45, 50 and 55 °C [17]. According to the above results, it is obvious that the CPT of alloy lies between 40 and 45 °C.

3.4. Potentiostatic CPT determination

In the potentiostatic method the higher potential is provided by using external source. Fig. 4 shows the anodic current density record during testing of the sample at the anodic potential of the 750 mV/SCE in the simulated solution. As it can be observed, the current density at the start of test starts decreasing until an integrated passive film covers the whole surface. After that, it decreases with a very low rate and background passivity current density reaches a value of almost 3 μA cm^{-2} indicates the healing of formed passive film on the surface [28]. In this step, there are some fluctuations indicating occurrence of metastable pitting [29–32].

By rising the temperature, another factor affects the passive film and it is the driving force for passivity dissolution and breakdown. At 39 °C, the background current density starts to increase and some small fluctuations are observed. These fluctuations may be as a result of raising the frequency of metastable pitting events or unavoidable noise during the test. This trend continues up to the temperatures of 41 °C at which the current density started to increase which is indicating the initiation of the pitting

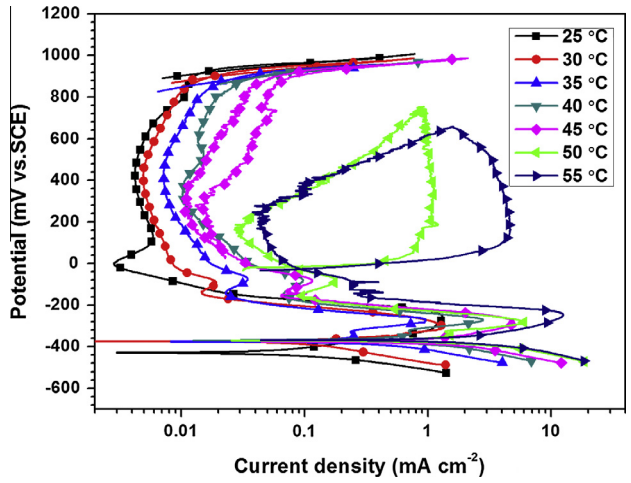

Fig. 3. Potentiodynamic polarisation method employed for determination of CPT of DSS2205.

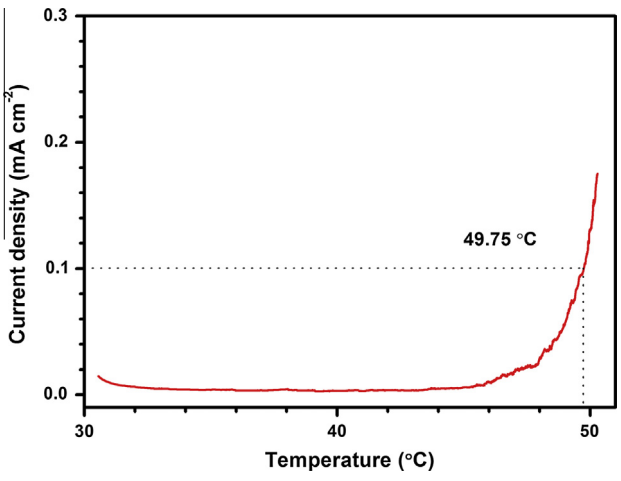

Fig. 4. Potentiostatic polarisation method used for CPT determination.

corrosion. In this way by considering the 100 μA cm^{-2} current density as a criterion for CPT evaluation, it can be seen that the CPT of the sample was 49.75 °C in simulated solution.

According to the obtained results, the CPT value determined by this method in the simulated solution is slightly higher than the CPT value measured by potentiodynamic, ASTM G 48 and ZRA methods. This may be attributed to the formation an integrated passivity on the entire surface that modifies by further increase in temperature below the CPT. Hence, the breakdown of thicker passive film occurs at slightly higher temperatures [28,33,34]. This explanation does not completely justify this observation because the CPT is a phenomenon which is highly related to the propagation process rather than initiation [18,29]. However, the main reason is that the current density starts an increasing trend from 41 °C (pit initiation stage) but it reaches the criterion (0.1 mA cm^{-2}) at 49.75 °C.

3.5. EIS CPT determination

Fig. 5 shows the nyquist and bode plots of the sample in the acidified $FeCl_3$ solution at different temperatures. The diagram shows that EIS results in the acidified $FeCl_3$ solution contain one time constant up to 45 °C and by increase in temperature, the decrease in the diameter of depressed semi-circle is obvious. This changes are also clear in bode plot which by increasing the temperature from 25 °C to 40 °C, impedance value at 1 Hz decreases from almost 9000–5000 Ω cm^2.

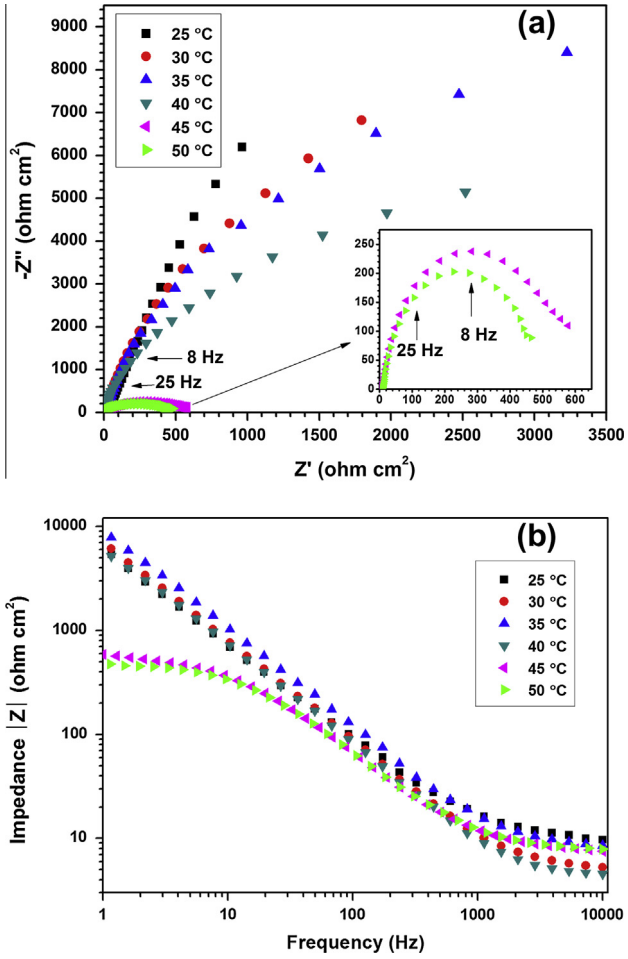

Fig. 5. (a) Nyquist plots for different temperatures regarding the proposed test condition for the new method and (b) corresponding impedance results.

However, as it can be seen, at temperature of 45 °C the diameter of the depressed semi-circle in nyquist plot and also the impedance value (|Z|) at the frequency of 1 Hz in bode plot decreased significantly. According to the previous work [20], this remarkable decrease in impedance value or diameter of Nyquist plot is an indication of pitting corrosion. The inserted graph in Fig. 5 shows the Nyquist plots for 45 and 50 °C indicating a significant decrease in charge transfer resistance from 25 °C to 50 °C. This is also clear that impedance value decreases from almost 5000–600 Ω cm^2 when temperature increases only 5 °C. This phenomenon can only be described by passivity breakdown and localized corrosion.

Fig. 6 shows the equivalent circuits used for modelling of the obtained results. In the presented models, equivalent circuit below the CPT differs with equivalent circuit above the CPT. This is because of the change in the surface condition of sample before and after pitting corrosion. As it can be seen, before pitting corrosion the circuit shows a randle-like feature related to the passive surface. However, after pitting corrosion, there are two different sites, passive area and pitted ones. The model in Fig. 6b can successfully simulate this condition. The more detailed description about this model can be found elsewhere [20].

Regarding to the Nyquist plots, it is obvious that the semi circles are depressed therefore, in these models constant phase elements (CPE) is used for more accurately analysing of impedance behaviour of the electric double layer. The impedance of CPE is expressed as [35]:

$$Z_{CPE} = P^{-1} \cdot (i\omega)^{-n} \quad (1)$$

where P is the magnitude of the CPE, ω is the angular frequency and n is the deviation parameter ($0 \leqslant n \leqslant 1$). For a circuit including a CPE, the double layer capacitance can be calculated from CPE parameters values (P and n) using the following expression [20].

$$C_{pass} = P^{\frac{1}{n}} \cdot R_{ct}^{\frac{1-n}{n}} \quad (2)$$

Table 2 demonstrates the obtained results from EIS test. As it can be seen, values of solution resistance (R_s) for all temperatures are close and similar and their value comparing to other resistances presented here is negligible.

The results reveal that there is a significant decrease in passivity resistance (R_{pass}) by raising the temperature. This parameter has value of 45,481 Ω cm^2 at 25 °C and decreases to 27,236 Ω cm^2 at 40 °C. It is remarkable to notice that there is no stable pitting corrosion up to 40 °C. As a result, this significant decline in this value illustrates the deteriorative effect of temperature on passivity condition as it was previously shown in potentiodynamic and potentiostatic polarisation results [22–25]. This is even obvious after occurring pitting corrosion in which the passivity resistance keeps its falling trend to 50 °C.

The reason for this notable decrease in passivity resistance is either decrease in its thickness or increase in the passivity film defects or both of them simultaneously. According to MacDonald, the reaction that causes passive film thickness to reduce is as follows [36]:

$$MO_{\frac{x}{2}} + xH^+ \rightarrow M^{d+}_{(aq)} + \frac{x}{2}H_2O + (\delta - x)e^- \quad (3)$$

where $MO_{x/2}$ represents passive oxide, x is mole number of protons involving in the reaction and δ is oxidation number of cation.

This reaction can be promoted by raising the temperature; resulting more dissolution of passive film. Nevertheless, temperature raising for the following reaction by which the passive film thickness remains constant leads to increase in cation vacancies and more defected passive film.

$$M_M \rightarrow M^{\delta+}_{(aq)} + V_M^{x-} + (\delta - x)e^- \quad (4)$$

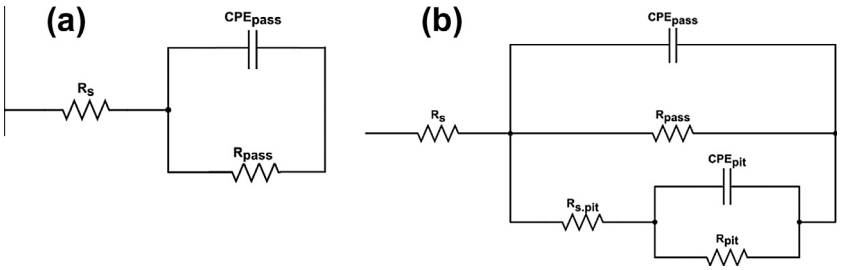

Fig. 6. Equivalent circuits used for modelling the EIS results (a) passive condition below CPT and (b) above CPT.

Table 2
Results of EIS method used for CPT determination.

T (°C)	R_s (Ω cm^2)	R_{pass} (Ω cm^2)	CPE_{pass} parameters		C_{pass} (μF cm^{-2})	$R_{s.pit}$ (Ω cm^2)	R_{pit} (Ω cm^2)	CPE_{pit} parameters		C_{pit} (μF cm^{-2})
			P (μF cm^{-2})	n				P (μF cm^{-2})	n	
25	14	45,481	20.3	0.99	20.33	–	–	–	–	–
30	10	39,667	23.84	0.94	23.76	–	–	–	–	–
35	12	38,244	23.93	0.93	23.77	–	–	–	–	–
40	7	27,236	32.58	0.88	32.05	–	–	–	–	–
45	8	24,101	26.94	0.95	26.33	124	654	466	0.17	1.41
50	10	21,326	31.71	0.94	30.98	76	560	502	0.16	0.63

In this reaction, M_M represents the atom in passive film and V_M^{x-} is cation vacancy as a result of removal of atom from the oxide. The values of C_{pass} clearly show an increasing trend by raising the temperature. By considering the Helmholtz model of the surface film capacitance, it is defined that the capacitance is inversely proportional to the surface film thickness [20].

$$C_{pass} = \frac{\varepsilon_0 \varepsilon}{d} S \tag{5}$$

where d is the thickness of the film, S is the surface of the electrode, ε_0 is the permittivity of the air, and ε is the local dielectric constant.

Since S and ε_0 are constant before pitting corrosion, any changes in C_{pass} come from either change in d or ε variation [24,25]. According to MacDonald [36], ε is constant over the range of passivity at constant temperature, however its variation with temperature is definitely probable considering the fact that temperature has a noticeable influence on fraction of vacancies in passive film either in the form of cation or anion vacancies.

This is noticeable that when pitting corrosion occurs, the surface condition changes and as a results, C_{pass} cannot be compared with those of non-pitting condition. The reason is that in the pitting condition surface area changes as well as other parameters mentioned above. In this condition, the passivated surface is lower compared to the non-pitting condition due to active corrosion of pitted area. However, clearly, even in pitting condition, C_{pass} increases with raising the temperature.

Based on the results of Table 2, similar explanation for the pitted area of samples at 45 °C and 50 °C can be said. It can be seen that the value for pit solution resistance decreases with the increase of temperature. This change may have some explanations. Firstly, there may be higher number of pits or bigger pits at 50 °C compared to 45 °C. Secondly, the rate of dissolution in this temperature is higher leading higher amount of ions and resulting lower resistance. Similar interpretations for changing in pit resistance and C_{pit} can be presented like those of passive state that are not brought here for avoiding duplication.

According to presented circuits, (neglecting the solution resistance which is almost constant in all tests) at temperatures lower than the CPT, the value of R_{total} is equal to R_{pass}, whereas at temperatures above the CPT, R_{total} is calculated by the following equation:

$$R_{total} = \frac{(R_{s.pit} + R_{pit}) \cdot R_{pass}}{(R_{s.pit} + R_{pit} + R_{pass})} \tag{6}$$

where R_{pass} is charge transfer resistance of the passive layer while $R_{s.pit}$ and R_{pit} are solution and charge resistance of the pit, respectively.

Fig. 7 shows the change in R_{total} values vs. temperature. In the case of EIS method the CPT can be considered as the temperature in which R_{total} value decreases sharply due to stable pitting formation. In addition, the CPT can be also defined as the temperature at which impedance value, $|Z|$, decreases significantly. Indeed, The CPT value of the sample lies between 40 to 45 °C which is in good correlation with the results obtained by other technique i.e. ZRA and potentiodynamic polarisation methods. This figure also reports the changes in breakdown potential from potentiodynamic polarisation vs. temperature. As it can be seen, the sharp decrease in E_b vs. T is observed in the temperature range of 45–50 °C. However, based on the discussions of the potentiodynamic polarisation results, pitting corrosion was initiated at the temperature of 45 °C, while the breakdown potential was not dropped significantly. As a result, the temperature range for the CPT is completely similar to the EIS results i.e. 40–45 °C.

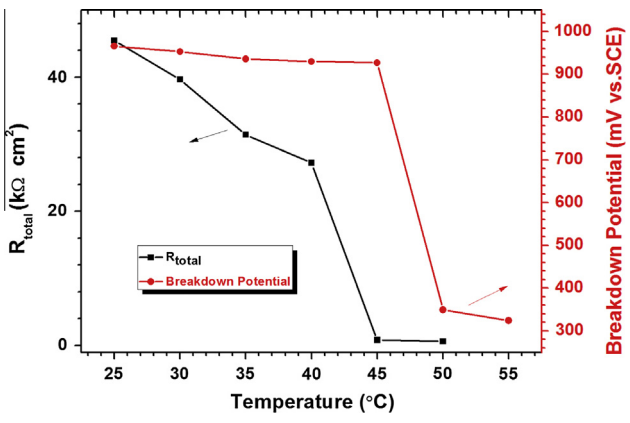

Fig. 7. Changing R_{total} and breakdown potential vs. temperature.

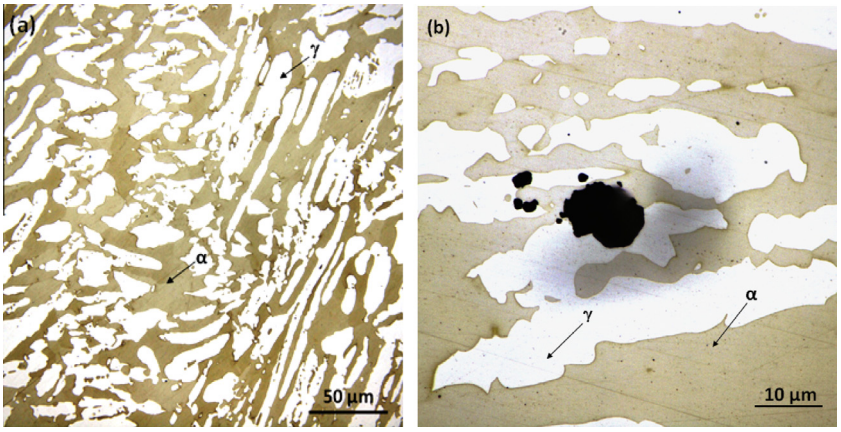

Fig. 8. Optical micrographs of (a) the base metal and (b) the created pits on the surface after 1 h in the ferric chloride solution at 55 °C. The ferrite (α) phase appears darker than austenite (γ) phase in the micrographs.

As it was mentioned before, the aim of this study was to introduce an alternative method of CPT measurement using EIS method. Ebrahimi et al. used EIS method successfully for this goal [20]. However, in their work, they applied an anodic DC potential and simultaneously employed EIS technique. In this work, higher potential was obtained using the method proposed in ASTM G 48 i.e. changing the solution chemistry and naturally locating the steel in passive region.

Based on the obtained results from different methods and results of this alternative method presented in Fig. 5 and Table 2, EIS can be used as another alternative method to determine CPT value of the stainless steels in ferric chloride solutions. Considering all methods, it is obvious that all of them give close temperatures for the CPT of this alloy. The changes between the results can be attributed to the nature of the test. In some of them like potentiostatic polarisation the surface passivity experiences some healing phenomena before pitting corrosion however, in some other pitting occurs more feasibly like standard one.

In this proposed method, there is no strong healing phenomena like potentiostatic polarisation that raise the incubation time for pitting corrosion. However, since the lower frequency is 1 Hz, this is a fast method that gives numerous valuable data related to the passivity and pitting conditions. In summary, using oxidant solutions and applying AC signals at high frequencies results to the fast and reliable determination of the CPT.

3.6. Pit morphology

Fig. 8a shows the microstructure of the DSS2205. Electrochemically etching the steel with KOH solution appears to darken the ferrite phase more than the austenite phase [12,37]. As it can be seen, the base metal has been composed of the almost equal amount of the each phase which is the favourable balance for this type of stainless steels. Fig. 8b shows the location of the stable pits after immersion in ferric chloride solution at the temperature of the 55 °C after 1 h. It is obvious that the pitting has been occurred in mainly austenite phase. It refers to the lower pitting resistance equivalent number (PREN) of the austenite phase compared to the ferrite phase which makes it more susceptible to pitting corrosion [12,37,38].

4. Conclusions

In this study a new alternative method for determination of CPT values of the stainless steels in ferric chloride solutions based on EIS method has been proposed and the following results were obtained:

1. The CPT values determined by ZRA and ASTM G 48 in acidified ferric chloride solutions were 42 °C and 40 °C, respectively.
2. The CPT values determined in simulated solution were 49.75 °C for potentiostatic polarisation and at the temperatures between 40 and 45 °C for potentiodynamic polarisation method.
3. The CPT values of the stainless steels in oxidant solutions containing aggressive ions such as Cl^- can be easily obtained by EIS method. In this case, at the temperatures above the CPT, the charge transfer resistance decreases significantly.
4. The CPT value determined by EIS method in ferric chloride solution is between 40 and 45 °C which is close to the values determined by the ZRA and potentiodynamic polarisation method.

Acknowledgment

Authors would like to appreciate the financial support from Ferdowsi University of Mashhad provision of laboratory facilities during the period that this research was conducted.

References

[1] R.J. Brigham, E.W. Tozer, Temperature as a pitting criterion, Corrosion 29 (1973) 33–36.
[2] R. Brigham, Effect of Cr on the pitting resistance of austenitic stainless steels, Corros. Sci. 15 (1975) 579–580.
[3] R.J. Brigham, Pitting of molybdenum bearing austenitic stainless steel, Corrosion 28 (1972) 177–179.
[4] R.J. Brigham, E.W. Tozer, Effect of alloying additions on the pitting resistance of 18% Cr austenitic stainless steel, Corrosion 30 (1974) 161–166.
[5] Y. Jiang, H. Tan, Z. Wang, J. Hong, L. Jiang, J. Li, Influence of Creq/Nieq on pitting corrosion resistance and mechanical properties of UNS S32304 duplex stainless steel welded joints, Corros. Sci. 70 (2013) 252–259.
[6] R. Qvarfort, Some observations regarding the influence of molybdenum on the pitting corrosion resistance of stainless steels, Corros. Sci. 40 (1998) 215–223.
[7] B. Deng, Z. Wang, Y. Jiang, H. Wang, J. Gao, J. Li, Evaluation of localized corrosion in duplex stainless steel aged at 850 °C with critical pitting temperature measurement, Electrochim. Acta 54 (2009) 2790–2794.
[8] N. Ebrahimi, M.H. Moayed, A. Davoodi, Critical pitting temperature dependence of 2205 duplex stainless steel on dichromate ion concentration in chloride medium, Corros. Sci. 53 (2011) 1278–1287.
[9] F. Eghbali, M.H. Moayed, A. Davoodi, N. Ebrahimi, Critical pitting temperature (CPT) assessment of 2205 duplex stainless steel in 0.1 M NaCl at various molybdate concentrations, Corros. Sci. 53 (2011) 513–522.
[10] L.F. Garfias-Mesias, J.M. Sykes, C.D.S. Tuck, The effect of phase compositions on the pitting corrosion of 25 Cr duplex stainless steel in chloride solutions, Corros. Sci. 38 (1996) 1319–1330.
[11] M.H. Moayed, N.J. Laycock, R.C. Newman, Dependence of the critical pitting temperature on surface roughness, Corros. Sci. 45 (2003) 1203–1216.

[12] H. Tan, Y. Jiang, B. Deng, T. Sun, J. Xu, J. Li, Effect of annealing temperature on the pitting corrosion resistance of super duplex stainless steel UNS S32750, Mater. Charact. 60 (2009) 1049–1054.
[13] P. Ernst, R.C. Newman, Explanation of the effect of high chloride concentration on the critical pitting temperature of stainless steel, Corros. Sci. 49 (2007) 3705–3715.
[14] ASTM G 150, Standard Test Method for Electrochemical Critical Pitting Temperature Testing of Stainless Steels, USA, West Conshohocken, 1999.
[15] ASTM G 48, Standard Test Methods for Pitting and Crevice Corrosion Resistance of Stainless Steels and Related Alloys by Use of Chloride Solution, USA, West Conshohocken, 2003.
[16] K. Vu Quang, P. Le Guevel, N. Jallerat, J. Bavay, Fast method for determination of critical pitting temperature, Corros. Sci. 28 (1988) 423–424.
[17] R. Ovarfort, Critical pitting temperature measurements of stainless steels with an improved electrochemical method, Corros. Sci. 29 (1989) 987–993.
[18] V.M. Salinas-Bravo, R.C. Newman, An alternative method to determine critical pitting temperature of stainless steels in ferric chloride solution, Corros. Sci. 36 (1994) 67–77.
[19] T. Zhang, D. Wang, Y. Shao, G. Meng, F. Wang, A new criterion to determine the critical pitting temperature (CPT) based on electrochemical noise measurement, Corros. Sci. 58 (2012) 202–210.
[20] N. Ebrahimi, M. Momeni, A. Kosari, M. Zakeri, M.H. Moayed, A comparative study of critical pitting temperature (CPT) of stainless steels by electrochemical impedance spectroscopy (EIS), potentiodynamic and potentiostatic techniques, Corros. Sci. 59 (2012) 96–102.
[21] Q.W. Knapp, J.C. Wren, Film formation on type-316L stainless steel as a function of potential: probing the role of gamma-radiation, Electrochim. Acta 80 (2012) 90–99.
[22] S.J. Ahn, H.S. Kwon, Effects of solution temperature on electronic properties of passive film formed on Fe in pH 8.5 borate buffer solution, Electrochim. Acta 49 (2004) 3347–3353.
[23] R.M. Carranza, M.G. Alvarez, The effect of temperature on the passive film properties and pitting behaviour of a Fe–Cr–Ni alloy, Corros. Sci. 38 (1996) 909–925.
[24] D.G. Li, Y.R. Feng, Z.Q. Bai, J.W. Zhu, M.S. Zheng, Influence of temperature, chloride ions and chromium element on the electronic property of passive film formed on carbon steel in bicarbonate/carbonate buffer solution, Electrochim. Acta 52 (2007) 7877–7884.
[25] H. Zhang, Y.L. Zhao, Z.D. Jiang, Effects of temperature on the corrosion behavior of 13Cr martensitic stainless steel during exposure to CO_2 and Cl^- environment, Mater. Lett. 59 (2005) 3370–3374.
[26] P.D. Bilmes, C.L. Llorente, C.M. Méndez, C.A. Gervasi, Microstructure, heat treatment and pitting corrosion of 13CrNiMo plate and weld metals, Corros. Sci. 51 (2009) 876–881.
[27] A. Pardo, M.C. Merino, A.E. Coy, F. Viejo, R. Arrabal, E. Matykina, Pitting corrosion behaviour of austenitic stainless steels – combining effects of Mn and Mo additions, Corros. Sci. 50 (2008) 1796–1806.
[28] S.-I. Pyun, M.-H. Hong, A model describing the growth kinetics of passivating oxide film prepared under potentiostatic conditions, Electrochim. Acta 37 (1992) 327–332.
[29] N.J. Laycock, M.H. Moayed, R.C. Newman, Metastable pitting and the critical pitting temperature, J. Electrochem. Soc. 145 (1998) 2622–2628.
[30] M.H. Moayed, R.C. Newman, Evolution of current transients and morphology of metastable and stable pitting on stainless steel near the critical pitting temperature, Corros. Sci. 48 (2006) 1004–1018.
[31] G.S. Frankel, L. Stockert, F. Hunkeler, H. Boehni, Metastable pitting of stainless steel, Corrosion 43 (1987) 429–436.
[32] P.C. Pistorius, G.T. Burstein, Metastable pitting corrosion of stainless steel and the transition to stability, Philos. Trans. R. Soc. London, Ser. A 341 (1992) 531–559.
[33] K.N. Goswami, R.W. Staehle, Growth kinetics of passive films on Fe, Fe–Ni, Fe–Cr, Fe–Cr–Ni alloys, Electrochim. Acta 16 (1971) 1895–1907.
[34] C.O.A. Olsson, D. Landolt, Passive films on stainless steels—chemistry, structure and growth, Electrochim. Acta 48 (2003) 1093–1104.
[35] N.S. Ayati, S. Khandandel, M. Momeni, M.H. Moayed, A. Davoodi, M. Rahimizadeh, Inhibitive effect of synthesized 2-(3-pyridyl)-3,4-dihydro-4-quinazolinone as a corrosion inhibitor for mild steel in hydrochloric acid, Mater. Chem. Phys. 126 (2011) 873–879.
[36] D.D. Macdonald, The point defect model for the passive state, J. Electrochem. Soc. 139 (1992) 3434–3449.
[37] Z. Zhang, D. Han, Y. Jiang, C. Shi, J. Li, Microstructural evolution and pitting resistance of annealed lean duplex stainless steel UNS S32304, Nucl. Eng. Des. 243 (2012) 56–62.
[38] B. Deng, Y.M. Jiang, J. Gao, J. Li, Effect of annealing treatment on microstructure evolution and the associated corrosion behavior of a super-duplex stainless steel, J. Alloys Compd. 493 (2010) 461–464.